NISTIR 4886

Implicitly Coupling Heat Conduction into a Zone Fire Model

William F. Moss
Glenn P. Forney

NIST United States Department of Commerce
Technology Administration
National Institute of Standards and Technology

NISTIR 4886

Implicitly Coupling Heat Conduction into a Zone Fire Model

William F. Moss
Clemson University
Clemson, SC 29634

Glenn P. Forney
Building and Fire Research Laboratory
Gaithersburg, MD 20899

July 1992

U.S. Department of Commerce
Barbara Hackman Franklin, *Secretary*
Technology Administration
Robert M. White, *Under Secretary for Technology*
National Institute of Standards and Technology
John W. Lyons, *Director*

Contents

List of Figures

List of Tables

Implicitly Coupling Heat Conduction into a Zone Fire Model

William F. Moss* Glenn P. Forney†

Abstract

This report examines several methods for coupling the partial differential equations that arise in conductive heat transfer with the ordinary differential equations that arise in zone fire modeling. Two existing algorithms (method of lines and time splitting) are discussed and a new strategy is proposed for performing this coupling. This strategy couples the wall surface temperature rather than the entire wall temperature profile with the other zone fire modeling solution variables by requiring that the wall surface temperature gradient and the incident heat flux (sum of convective and net radiative flux) satisfy Fourier's law, $q'' = -K\partial u/\partial x$.

Two prototype fire models were written to test the ideas discussed in this report. The first, CONRAD1, implements the method of lines strategy for solving heat conduction. The second, CONRAD2, implements the new strategy. Though inefficient, CONRAD1 uses well established numerical techniques and therefore serves as a benchmark to test the numerical ideas implemented in CONRAD2. Both programs use the stiff differential-algebraic equation solver DASSL. Supporting numerical results are presented.

1 Introduction

In a zone fire model, each room in a building is divided into a relatively smoke-laden upper layer and a relatively clear lower layer. Temperatures in the ceiling, floor, and vertical walls of a room must be computed in order to adequately account for heat

*Department of Mathematical Sciences, Clemson University, Clemson, SC 29634–1907, U.S.A. (bmoss@math.clemson.edu).

†Building and Fire Research Laboratory, National Institute of Standards and Technology, Gaithersburg, MD 20899, U.S.A. (gpfrn@cfr6.cfr.nist.gov).

exchange due to convective and radiative heat transfer. The ceiling, floor, and vertical walls of each room are usually divided into "wall" segments. Here the term "wall" may mean the ceiling, the floor, or the vertical walls of a room. Wall temperatures are usually computed by solving a series of 1-d heat conduction problems; one problem per wall segment. The gas layers in a zone fire model are often modeled using ordinary differential equations (ODE) which are derived from conservation of mass and energy. CCFM.VENTS [1] and FAST (renamed CFAST) [2] are two examples of zone fire models. CCFM.VENTS uses pressure, layer interface height, and upper and lower layer masses as solution variables, while CFAST uses pressure, upper layer volume, and upper and lower layer temperatures. Reference [3] shows how these two and many other formulations are equivalent in the sense that one can be converted into another using the ideal gas law and definitions of physical properties such as internal energy and density.

The heat conduction problems for the wall segments are formulated using the heat conduction equation, a partial differential equation (PDE) [4], which can be derived using the conservation of energy. The gas solution variables and the wall segment temperature profiles are presumed known at some time t. The ODE's and PDE's are used to advance the solution variables to some later time $t + \Delta t$. The gas layers and the wall segments or equivalently the ODE's and the PDE's are coupled *via* convective and radiative heat transfer terms.

Procedures for solving 1-d heat conduction problems are well known. For finite difference methods such as backward difference (fully implicit), forward difference (fully explicit) or Crank-Nicolson see [5]. For finite element methods see [6].

The question addressed by this report is how to couple the ODE's from the gas layers with the PDE's from the wall segments in a numerically accurate, robust and efficient manner.

Two prototype fire codes were written to test the ideas presented in this report. CONRAD1 implements the method of lines strategy for solving the heat equation using standard cubic Hermite polynomials to represent the unknown wall temperature profile. CONRAD2 implements a new method called "gradient matching" which is based on an implicitly defined functional equation approach. Though inefficient, CONRAD1 uses well established numerical techniques and therefore serves as a benchmark to test the new numerical ideas implemented in CONRAD2. CONRAD1 and CONRAD2 both use the stiff differential-algebraic equation (DAE) solver DASSL[7, 8]. These zone fire models, documented in [9], use the same solution variables as CCFM.VENTS which are denoted by P, y, m_U and m_L. Here these variables are referred to as the gas solution variables. The procedures discussed in this report for coupling the gas zone properties with the wall temperatures will work for many other formulations of the gas solution variables.

2 Background

Two standard approaches for coupling zone fire modeling differential equations with 1-d heat conduction problems are time splitting and the method of lines (MOL). These two methods will be briefly discussed in the next two subsections.

2.1 Time Splitting

Time splitting makes the assumption that two or more phenomena change over significantly different time scales. For example, in the zone fire modeling case, it can often be assumed that the characteristic time scale for wall segment temperature profiles is much longer than that for the gas solution variables. Suppose that the gas solution variables and the wall segment temperature profiles are known at time t. If the characteristic time scale for wall segment temperature profiles is Δt, then wall segment temperature profiles would be solved over the time interval $(t, t + \Delta t)$. This time interval would then be further subdivided in order to solve for the shorter time scale phenomena. The longer time interval is often called the outer time step and the shorter interval is called the inner time step.

Referring to Figure 1, time splitting advances the short time scale phenomena from time t to time $t+\Delta t$ in a series of time steps chosen sufficiently small by the solver to satisfy the error criteria. Next the wall segment temperature profiles, are advanced from time t to time $t + \Delta t$. The outer time stepsize Δt must be chosen sufficiently small so that the computed wall segment temperature profiles are consistent with the gas solution variables at time $t + \Delta t$. By consistent it is meant that the heat flux striking each wall segment, q'', is related to the temperature gradient, $\partial u/\partial x$, at the surface of the wall segment *via* Fourier's law, $q'' = -K\partial u/\partial x$, where K is the thermal conductivity of the wall.

The wall segment temperature profiles are advanced using a flux boundary condition. The flux at the interior surface of a wall segment is the sum of convective and net radiative heat fluxes. The question then is what flux to use to advance the solution; the flux at time t, the flux at time $t + \Delta t$, or some combination. The flux at time $t + \Delta t$ is not known until both the inner variables (P, y, m_U and m_L) and the outer variables (wall segment temperature profiles) are determined at $t + \Delta t$. Consequently, an iterative procedure must be used to insure that the flux striking the interior surface of a wall segment is consistent with the temperature gradient there.

The method of time splitting does not work well when the time scales are close which can occur when wall materials are thin and/or highly conductive. Time splitting is also difficult to implement efficiently since it is not clear what time stepsizes should be used. A time stepsize chosen too small will result in inefficiency and time stepsize chosen too large will result in unnecessarily inaccurate answers. The former

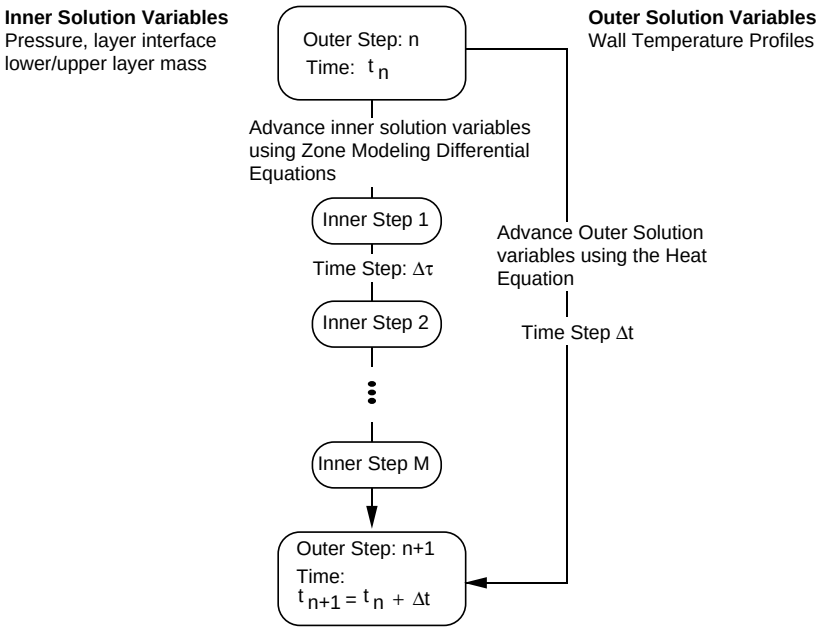

Figure 1: A General Flowchart for the Method of Time Splitting

can easily occur as a fire simulation approaches steady state. In this case, solution variables do not change much and inefficiency occurs because of restrictive time step-size selections.

2.2 Method of Lines

The MOL consists of converting the heat conduction partial differential equation into a system of ordinary differential equations. The unknown wall segment temperature profile is expanded as

$$\hat{u}(x,t) = \sum_{k=1}^{N} a_k(t) B_k(x) \tag{1}$$

where $\hat{u}(x,t)$ is an approximation to the unknown temperature profile at a distance x into the wall segment at time t. The functions $B_k(x)$ are known basis functions and the $a_k(t)$ are unknown coefficient functions. Equation (1) is substituted into the heat equation

$$\frac{\partial u(x,t)}{\partial t} = \alpha \frac{\partial^2 u(x,t)}{\partial x^2} \ ,$$

where α is the thermal diffusivity, to obtain a differential equation for the unknown coefficients a_k:

$$\sum_{k=1}^{N} a_k'(t) B_k(x) = \alpha \sum_{k=1}^{N} a_k(t) B_k''(x) \ .$$

A system of ODE's is obtained by requiring that the above equation be satisfied at a set of collocation points $x = x_1, \ldots, x_{N-2}$. The flux boundary conditions at each end of the wall segment generate two additional equations. Many variations of the MOL algorithm can be derived by choosing different basis functions (B-Splines, cubic Hermite interpolating polynomials, trigonometric polynomials, for example) and different sets of collocation points. The MOL algorithm in CONRAD1 uses the standard basis functions for cubic Hermite polynomial interpolation, and it uses Gaussian points for collocation points. This is discussed in Appendix A.

In CONRAD1, the ODE's for the the gas solution variables and the coefficients a_k are solved simultaneously. Heat conduction and gas phenomena are coupled *via* radiative and convective heat transfer.

In CONRAD1 and CONRAD2 the four gas solution variables have four associated ODE's. In CONRAD1, the number of additional ODE's required per room is NM where N is the number of basis functions used to represent the wall segment temperature profiles and M is the number of wall segments per room. Even for moderate

values of M, N, and the number of rooms, the run-times required for CONRAD1 can easily increase by an order of magnitude over a simulation with the conduction submodel turned off.

CONRAD1 advances the gas solution variables along with the wall temperature profiles from time t to $t + \Delta t$. The time stepsize, Δt, is chosen by the DAE solver to satisfy appropriate error criteria. The flux boundary conditions form part of the system of equations being solved. As a result, the inconsistencies that could arise using time splitting will not occur. This gain in consistency, however, is at the expense of increased computational requirements.

As is the case here, the MOL often requires a DAE solver because the boundary conditions are algebraic equations which cannot be easily converted into ODE's. For simple problems in which the boundary conditions can be easily differentiated with respect to time, a standard (stiff) ODE solver can be used.

3 Coupling Heat Conduction Using Gradient Matching

This report presents a new strategy for coupling 1-d heat conduction problem with the ODE's for the gas solution variables. Only the temperature of the interior wall segment surface (as opposed to the entire wall segment temperature profile) is directly coupled with the gas layers and fire through convective and radiative heat transfer. This observation has been exploited to design a new and efficient algorithm for coupling heat conduction with a zone fire model.

3.1 Description

The method for modeling heat conduction discussed in this section couples the wall segment surface temperatures, rather than the entire wall segment temperature profile, with the gas solution variables by requiring that the wall segment surface temperature gradient, $\frac{\partial u(x,t)}{\partial x}$, and the incident heat flux (sum of convective and net radiative flux), q'' satisfy Fourier's law

$$q'' = -K\frac{\partial u(x,t)}{\partial x} \tag{2}$$

at the wall boundaries $x = 0$ and $x = W$ where K is the thermal conductivity of the wall material and W is the wall thickness. This solution strategy requires a DAE solver that can simultaneously solve both differential (gas ODE's) and algebraic equations (Fourier's law). With this method, only one or two extra equations are required per wall segment (two if both the interior and exterior wall segment surface temperatures are computed). This solution strategy is computationally more efficient

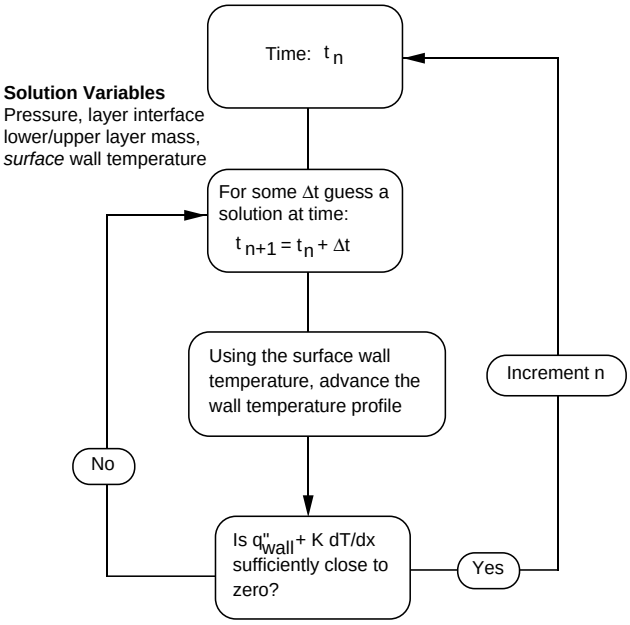

Figure 2: A General Flowchart for the Method of Gradient Matching

than the method of lines since fewer equations need to be solved. Wall segment temperature profiles, however, still have to be stored so there is no decrease in storage requirements.

Consider a room with a single wall segment with both interior and exterior wall segment surface temperatures computed. In this case, there will be six solution variables, the four gas solution variables, P, y, m_U, m_L, plus the two wall segment surface temperatures. There will be six equations to solve, four ODE's associated with the gas solution variables, plus two algebraic equations consisting of Fourier's law applied at the surfaces of the wall segment. Referring to Figure 2, the gradient matching method assumes that the gas solution variables and the wall segment temperature profile are known at time t. The DAE solver will make an initial guess at values for the solution variables at time $t + \Delta t$. Based on the wall segment surface temperatures at times t and $t + \Delta t$, the wall segment temperature profile is advanced to time $t + \Delta t$. Next, the wall segment surface temperature gradients are estimated at time $t + \Delta t$. Finally, the residuals are computed at time $t + \Delta t$ for the six equations including the two Fourier law equations. The DAE solver adjusts the stepsize Δt until the residuals for all six equations are below an error tolerance.

3.2 Theoretical Justification for the Algorithm

The basic idea is to transform the initial-boundary value problem for each wall segment into a pair of functional equations. To explain further, consider the following standard problem. Find the temperature profile $u(x,t)$ that satisfies

$$\begin{aligned} \frac{\partial u(x,t)}{\partial t} &= \alpha \frac{\partial^2 u(x,t)}{\partial x^2},\ 0 < x < W,\ t > 0 && (3)\\ u(x,0) &= g(x),\ 0 \le x \le W && (4)\\ u(0,t) &= f_0(t),\ t \ge 0 && (5)\\ u(W,t) &= f_1(t),\ t \ge 0, && (6) \end{aligned}$$

where g, f_0, and f_1 are given continuous functions, $\alpha = \frac{K}{\rho c}$ is the thermal diffusivity, K is the thermal conductivity, ρ is the density and c is the specific heat of the wall material. The existence and uniqueness theory (see [10]) for this problem shows that $u(x,t)$ is uniquely determined by the initial temperature profile, g, and the interior and exterior temperature boundary functions $f_0(\tau)$ and $f_1(\tau)$ for $0 \le \tau \le t$. In other words, there is a functional relation between the initial temperature profile, boundary functions, and the solution of the form

$$u(x,t) = G[g, f_0(0 \le \tau \le t), f_1(0 \le \tau \le t)](x,t)\ . \tag{7}$$

In [10] the Laplace transform is used to construct the functional G. In the special case when the initial temperature is constant, say $u(x,0) = T_{\text{amb}}$, the functional G can be written in terms of convolution integrals. With $\alpha = W = 1$, the solution has the form

$$u(x,t) = T_{\text{amb}} - \int_0^t f_0(t-\tau)\frac{\partial}{\partial x}\theta_3(\frac{x}{2},\tau)d\tau - \int_0^t f_1(t-\tau)\frac{\partial}{\partial x}\theta_3(\frac{1-x}{2},\tau)d\tau\ ,$$

where $\theta_3(x,t)$ is a theta function [11] which can be expressed as

$$\theta_3(x,t) = 1 + 2\sum_{k=1}^{\infty} e^{-\pi^2 k^2 t}\cos 2\pi k x\ .$$

From equation (7), substituting $x = 0$ for the interior and $x = W$ for the exterior wall segment boundaries, it follows that

$$\begin{aligned} \frac{\partial u}{\partial x}(0,t) &= \frac{\partial}{\partial x}G[g, f_0(0 \le \tau \le t), f_1(0 \le \tau \le t)](0,t)\\ \frac{\partial u}{\partial x}(W,t) &= \frac{\partial}{\partial x}G[g, f_0(0 \le \tau \le t), f_1(0 \le \tau \le t)](W,t)\ . \end{aligned}$$

For each wall segment in a room, two functional equations are added to four gas ODE's. These equations, based on Fourier's law (equation (2)), have the form

$$K\frac{\partial}{\partial x}G[T_{\text{amb}}, u(0, 0 \le \tau \le t), u(W, 0 \le \tau \le t)](0, t) + q''(u(0,t), m_L(t), m_U(t), y(t), P(t)) = 0 \tag{8}$$

$$K\frac{\partial}{\partial x}G[T_{\text{amb}}, u(0, 0 \le \tau \le t), u(W, 0 \le \tau \le t)](W, t) + q''(u(W,t), m_L(t), m_U(t), y(t), P(t)) = 0\ . \tag{9}$$

The expressions $u(0, 0 \le \tau \le t)$ and $u(W, 0 \le \tau \le t)$ in equations (8) and (9) denote the temperatures of the interior and exterior wall segment surfaces over the time interval $(0, t)$ which makes these functional equations.

Returning to the one room, one wall segment discussion of the previous section, there are six unknowns: $P(t)$, $y(t)$, $m_L(t)$, $m_U(t)$, $u(0, t)$, and $u(W, t)$. Four ODE's for the first four unknowns are coupled with the two functional equations (8) and (9). The resulting system can be called a differential-functional equation (DFE) system. The gradient matching method is a procedure for finding an approximate solution to this DFE system using a DAE solver. It is based on the following semi-group property of the heat equation. The temperature profile obtained by advancing the initial profile to time $t + \Delta t$ is identical with the profile obtained by first advancing the initial profile to time t and then advancing it from time t to time $t + \Delta t$. Implementation of the gradient matching method requires that storage be allocated for the temperature profile at the previous time, t, and at the next time, $t + \Delta t$. Given the profile at time t and values for the six unknowns at time $t + \Delta t$ (initial guess by the solver), the profile G is advanced from time t to time $t + \Delta t$. The gradient of G at $x = 0$ and $x = W$ is computed followed by the residuals for the six equations including equations (8) and (9). The DAE solver adjusts the stepsize Δt until the residuals for all six equations are below an error tolerance. Once the solver has completed the step, the array storing the temperature profile for the previous time is updated, and the DAE solver is ready to take its next step.

3.3 Implementation Details

The gradient matching method was implemented in CONRAD2. For CONRAD2 the set of unknowns are constructed as follows. For each room in which conduction is modeled, there are four wall segments. The floor and ceiling are each treated as a segment. The vertical walls in the room are divided into two segments, one above the layer interface and one below. Each segment contributes two unknowns, one for the segment interior surface temperature and one for the segment exterior surface

temperature. The four gas solution variables P, y, m_U, and m_L bring the total number of unknowns to twelve per room.

To compute the first terms in equations (8) and (9) at time $t+\Delta t$, the temperature profile must be advanced from time t to time $t+\Delta t$ and its endpoint gradients approximated. To advance the temperature profile a simple MOL approach was used in CONRAD2. A graded (non-uniform) mesh with n_x breakpoints was introduced for the spatial variable x. The second spatial derivative in the heat equation was replaced by a second divided (finite) difference approximation. This produces a system of n_x-2 ODE's for the n_x-2 unknown temperatures at the interior breakpoints. This system was solved by one step of the backward Euler method. Crank-Nicholson was also tried but produced spurious oscillations in the temperature profiles at the beginning of the simulation; backward Euler does not suffer from this defect which is related to the non-uniform mesh being used. The solution at time $t+\Delta t$ can be found by solving a tridiagonal system of linear equations. The temperature gradient at $x=0$ and time $t+\Delta t$ was approximated by interpolating the temperature values at the first three breakpoints with a quadratic and then evaluating the derivative of this polynomial at $x=0$. A similar procedure was used to approximate the temperature gradient at $x=W$ and time $t+\Delta t$.

A graded mesh scheme was chosen to allow breakpoints to cluster near the interior and exterior wall segment surfaces. This is where the temperature gradients are the steepest. A breakpoint x_b was defined by $x_b = \min(x_p, W/2)$, where $x_p = 2\sqrt{\alpha t_{\text{final}}}\,\text{erfc}^{-1}(.05)$ and erfc^{-1} denotes the inverse of the complementary error function. The value x_p is the location in a semi-infinite wall where the temperature rise is 5% after t_{final} seconds; it is sometimes called the penetration depth. Eighty percent of the breakpoints were placed on the interior side of x_b and the remaining twenty percent were placed on the exterior side.

The temperature profile in a conduction node at time $t+\Delta t$ is found from the temperature profile at time t by solving a tridiagonal system as follows. Let $u_i(t)$ denote the approximate temperature at time t and breakpoint x_i, let $\Delta x_i = x_{i+1} - x_i$ denote the breakpoint spacing, and let $s = \frac{2\alpha\Delta t}{W^2}$. The tridiagonal system that must be solved is

$$\begin{pmatrix} 1 & 0 & & & & \\ b_2 & a_2 & c_2 & & & \\ & \ddots & & & & \\ & & b_{n_x-1} & a_{n_x-1} & c_{n_x-1} & \\ & & & 0 & 1 & \end{pmatrix} \begin{pmatrix} u_1(t+\Delta t) \\ u_2(t+\Delta t) \\ \vdots \\ u_{n_x-1}(t+\Delta t) \\ u_{n_x}(t+\Delta t) \end{pmatrix} = \begin{pmatrix} f_0(t+\Delta t) \\ u_2(t) \\ \vdots \\ u_{n_x-1}(t) \\ f_1(t+\Delta t) \end{pmatrix},$$

where for $i = 2, \ldots, n_x - 1$

$$\begin{aligned} a_i &= 1 + \frac{s}{\Delta x_{i-1} \Delta x_i} \\ b_i &= \frac{-s}{\Delta x_{i-1}(\Delta x_{i-1} + \Delta x_i)} \\ c_i &= \frac{-s}{\Delta x_i(\Delta x_{i-1} + \Delta x_i)} \; . \end{aligned}$$

If the spacing is uniform ($\Delta x_i = \Delta x$) and $s = \Delta x^2$ then the above coefficient matrix reduces to

$$\begin{pmatrix} 1 & 0 & & & & \\ -\frac{1}{2} & 2 & -\frac{1}{2} & & & \\ & \ddots & & & & \\ & & & -\frac{1}{2} & 2 & -\frac{1}{2} \\ & & & & 0 & 1 \end{pmatrix}$$

In wall materials composed of multiple slabs, a different form for a_i, b_i and c_i must be used at the breakpoints where the slab material properties change. This occurs because the second partial of temperature, $\frac{\partial^2 u}{\partial x^2}$, does not exist at these breakpoints. Formulas for these coefficients are derived in Appendix B using the fact that heat flow through a wall is continuous. These breakpoint coefficients are

$$\begin{aligned} a_i &= \frac{K_i^+}{\Delta x_i} - \frac{K_i^-}{\Delta x_{i-1}} \\ b_i &= -\frac{K_i^-}{\Delta x_{i-1}} \\ c_i &= \frac{K_i^+}{\Delta x_i} \\ d_i &= 0 \end{aligned}$$

where $K_i^+ (K_i^-)$ is the thermal conductivity on the right(left) side of breakpoint x_i.

The gradients at time $t + \Delta t$ at the points $x = 0$ and $x = W$ are estimated from quadratics passing through the first three and last three temperature values. These gradients are computed using Newton divided differences. Let $u(x_0)$, $u(x_1)$ and $u(x_2)$

denote the temperatures at the first three breakpoints. The wall temperature gradient at the interior surface is estimated by

$$K\frac{u[x_1,x_2]-u[x_1,x_2,x_3]\Delta x_1}{W}$$

where

$$\begin{aligned} u[x,y] &= \frac{u(x)-u(y)}{x-y}, \\ u[x,y,z] &= \frac{u[x,y]-u[y,z]}{x-z}. \end{aligned}$$

Similarly the wall temperature gradient at the exterior surface is given by

$$K\frac{u[x_{n_x-1},x_{n_x}]-u[x_{n_x-2},x_{n_x-1},x_{n_x}]\Delta x_{n_x-1}}{W}\ .$$

4 Numerical Results

In this section the MOL approach used in CONRAD1 is compared numerically with the gradient matching approach used in CONRAD2. These numerical experiments were conducted on a Sun Sparcstation 2. CONRAD1 and CONRAD2 were written in Fortran 77 together with two extensions that are available on almost all Fortran 77 compilers. These extensions are the "IMPLICIT NONE" statement that forces the typing of all variables and the "INCLUDE" statement that allows various header files to be read at the beginning of a program unit. CONRAD2 has been ported to and tested on an Apple Macintosh II, a Sun Sparcstation 2, a Silicon Graphics 4D35, and an IBM Risc 6000 Model 320. CONRAD1 has been ported to and tested on an Apple Macintosh II, a Sun Sparcstation 2, and a Silicon Graphics 4D35. The only machine dependent parts of these codes are the default unit number for screen output, the timing routines, and the floating point constants. CONRAD1 and CONRAD2 are fully documented *via* comment statements which include porting instructions.

The user communicates with CONRAD1 and CONRAD2 through nearly identical input data files. In this section, these codes are compared on a four room test case for which the CONRAD1 input data file has the following structure. The units here are meters and seconds.

```
'RELATIVE ERROR TOLERANCES FOR P, Y, MU, ML, NODETEMP, NODETEMPGRAD'
1.D-6  1.D-6  1.D-6  1.D-6 1.D-3 1.D-3
'ABSOLUTE ERROR TOLERANCES FOR P, Y, MU, ML, NODETEMP, NODETEMPGRAD'
1.D-6  1.D-6  1.D-6  1.D-6 0.D0  0.D0
```

```
'NUMBER OF ROOMS'
4
'FIRE WATTS,DIM:DATUM TO FLOOR,XROOM,YROOM,ZROOM,GXFIRE,GYFIRE,GZFIRE'
'FOLLOWED BY RADIATION,NODES,CODES(0=NULL,1=CONCRETE,2=GYPSUM,3=KAOWOOL)'
500000.  0.  3.64 3.63 2.45  0. 0. 0.
.TRUE.  4  2  2  2  2
     0.  0.  2.43 18.9 2.43  0. 0. 0.
.TRUE.  4  2  2  2  2
     0.  0.  3.64 3.65 2.45  0. 0. 0.
.TRUE.  4  2  2  2  2
     0.  0.  3.52 3.52 2.43  0. 0. 0.
.TRUE.  4  2  2  2  2
'NUMBER OF VENTS'
6
'AREA, DIS: DATUM TO TOP,DATUM TO BOTTOM,ROOM NUMBERS ON EACH SIDE'
 0.18400E+01  0.20000E+01 0.00000E+00    1  2
 0.50000E-01  0.30000E+00 0.20000E+00    1 -1
 0.60000E-01  0.20000E+01 0.00000E+00    2  3
 0.60000E-01  0.20000E+01 0.00000E+00    2  4
 0.50000E-01  0.30000E+00 0.20000E+00    3 -1
 0.50000E-01  0.30000E+00 0.20000E+00    4 -1
'NUMBER OF FORCED VENTS'
0
'AREA, DIS: DATUM TO TOP,DATUM TO VENT,FLOW RATE,ROOM NUMBERS ON EACH SIDE'
'TFINAL, TPRINT'
600.  60.
'LOGICAL, TS, TF: DIAGNOSTICS AT INTERMEDIATE STEPS IN INTERVAL [TS, TF]'
.FALSE.  0.0  0.5
'NUMBER OF BREAKPOINTS NX'
5
```

Lines 2 and 4 specify six error tolerances. For CONRAD2 the last tolerance is left out since wall segment temperature gradients are not solution variables in CONRAD2. Lines 10, 12, 14, and 16 specify that the radiation submodel should be used in each room, that four wall segments (nodes) should be used in each room, and that all wall segment materials should be gypsum. Lines 20–25 specify the vents that interconnect the rooms. Room number -1 indicates the outside. The last line specifies the number of breakpoints used in the wall segments. This number is 5 for CONRAD1 and 20 for CONRAD2. These numbers were chosen on the basis of a set of numerical experiments. Using more than this number of breakpoints does not significantly improve the accuracy of the wall segment temperature profile computation.

Table 1 gives cpu times in seconds for three cases: gas equations only, gas plus conduction equations, gas plus conduction plus radiation. The wall segment surface temperatures for these two codes agreed to within the error tolerance set in the input

Table 1: CPU Time Comparisons

Code	gas	gas + cond	gas + cond + rad
CONRAD1	3.1	45.2	97.5
CONRAD2	3.4	30.5	51.6

data file which here is 0.1%. This table illustrates the savings in cpu time provided by CONRAD2 without any loss of accuracy in the computation of wall segment temperatures. The number of DAE's solved by DASSL in CONRAD1 is 16 for the gas case and 176 for the gas plus conduction and gas plus conduction plus radiation cases. The number of DAE's solved by DASSL in CONRAD2 is 16 for the gas case and 48 for the gas plus conduction and gas plus conduction plus radiation cases. Notice that the cost of using the radiation submodel is significant.

No attempt has been made in CONRAD1 to exploit any special structure in the linear systems that DASSL solves at each time step. DASSL solves a nonlinear system at each time step by a variant of Newton's method. Each iteration of this method requires the solution of a linear system. The structure of the coefficient matrix of this linear system is dependent on the interconnectivity of the rooms. Consider an example in which four rooms are side by side with a vent connecting rooms 1 and 2, a vent connecting rooms 2 and 3, a vent connecting rooms 3 and 4, and a vent from room 1 to the outside. In this case, the coefficient matrix will have a band structure and the band solver provided with DASSL can be used. The minimum band width will occur when the rooms are in a "chain" as in this example. If each room is interconnected with all other rooms, this coefficient matrix will be full. Consequently, there is no easy way to exploit the structure of this coefficient matrix without making a priori assumptions about the interconnectivity of the rooms. On the other hand, each wall segment contributes a tridiagonal block to this coefficient matrix. Perhaps it would be possible to create a special solver that would be able to exploit this feature of the matrix. If CONRAD2 is later found to have limitations, then creating a special solver to use with DASSL in CONRAD1 might be worthwhile.

5 Future Work

The use of a DAE solver to solve a DFE system appears to be a new and useful development in the application of mathematics. The theoretical basis and the limitations

of this method will be further explored. This is a mathematical analysis issue, not a programming issue.

The subroutine CNDUCT in CONRAD2 which solves the heat equation for a wall segment can be rewritten based on a piecewise cubic Hermite expansion approach instead of the current finite difference approximation approach. This change has several advantages. The order of accuracy of the spatial approximation is increased, and consequently, fewer breakpoints and less memory are required. The expansion approach provides a natural method for interpolating the temperature profile between breakpoints, and it provides the gradients at the endpoints directly without the need for an additional approximation. The expansion approach should also be less sensitive to poorly chosen breakpoint spacing. The resulting linear system that must be solved is now pentadiagonal instead of tridiagonal, but the size of the system is cut in half.

The breakpoint heuristic in CONRAD2 can be improved. The current heuristic is based on the final time t_{final}. As an alternative, three different sets of breakpoints could be generated based on three times $t_{\text{short}} < t_{\text{mid}} < t_{\text{final}}$. Subroutine CNDUCT could be rewritten to use the set based on t_{short} for $0 < t \leq t_{\text{short}}$, the set based on t_{mid} for $t_{\text{short}} < t \leq t_{\text{mid}}$, and the set based on t_{final} for $t_{\text{mid}} < t \leq t_{\text{final}}$. This would amount to a crude moving mesh strategy. When the set of breakpoints is changed, the current temperatures at the new breakpoints must be computed. This is especially easy with the expansion approach since it provides a natural interpolation formula.

Currently, the ceiling and floor in a room are each treated as wall segments and the vertical walls are divided into two segments, one above the layer interface and one below the layer interface. Consequently, the two segments of the vertical walls have surface areas which change with time. The temperature distribution in the vertical walls can be more accurately modeled by using more than two segments with fixed surface areas, or by moving to a 2-d conduction model in the vertical walls. Currently, the exterior surfaces of the wall segments in CONRAD1 and CONRAD2 exchange heat to ambient. The model could be improved by allowing neighboring rooms to exchange heat *via* conduction through ceilings, walls, and floors. A simple first step would be to implement this for the room(s) of fire origin.

6 Summary

Two standard methods, time splitting and the method of lines, were presented for coupling the partial differential equations that arise when modeling heat conduction with the ordinary differential equations that arise in zone fire modeling. Effective time splitting implementations rely on the assumption that the time split phenomenon changes over a significantly longer time scale than other phenomena of interest. This assumption breaks down when wall materials are thin and/or highly conductive since

they react more quickly to changing boundary conditions. The method of lines does not have these problems. However, efficient implementations are difficult to attain due to the large number of extra ordinary differential equations that are introduced.

A third heat conduction coupling method, gradient matching, was introduced to address the above deficiencies. This method couples only the surface wall temperatures with the other gas solution variables. These are the temperatures that are of primary concern since only the wall surface temperatures (not the interior wall temperatures) interact with the gas layers (*via* convective and radiative heat transfer).

Numerical experiments were performed that demonstrated that the new scheme was not only more efficient (as implemented in CONRAD2) but agreed with established numerical methods (using the method of lines as implemented in CONRAD1) to within the numerical solver tolerance error of .1 per cent.

References

[1] Leonard. Y. Cooper and Glenn P. Forney. The consolidated compartment fire model (CCFM) computer application CCFM.VENTS - part i: Physical reference guide. Internal Report 4342, National Institute of Standards and Technology, 1990.

[2] Walter W. Jones and Richard D. Peacock. Technical reference guide for FAST version 18. Technical Note 1262, National Institute of Standards and Technology, 1989.

[3] Glenn P. Forney and William F. Moss. Analyzing and exploiting the numerical characteristics of zone fire models. Internal Report 4763, National Institute of Standards and Technology, 1992.

[4] Frank P. Incropera and David P. De Witt. *Fundamentals of Heat and Mass Transfer*. John Wiley and Sons, New York, third edition, 1990.

[5] Gene H. Golub and James M. Ortega. *Scientific Computing and Differential Equations, An Introduction to Numerical Methods*. Academic Press, New York, 1989.

[6] Gilbert Strang and George J. Fix. *An Analysis of the Finite Element Method*. Prentice Hall, Englewood Cliffs, New Jersey, 1973.

[7] K. E. Brenan, S. L. Campbell, and L. R. Petzold. *Numerical Solution of Initial-Value Problems in Differential-Algebraic Equations*. North-Holland, New York, New York, 1989.

[8] Linda R. Petzold. A description of DASSL: A differential/algebraic system solver. technical report 8637, Sandia National Laboratories, 1982.

[9] William F. Moss. Numerical analysis support for compartment fire modeling and incorporation of heat conduction into a zone fire model. Government Contract Report 605, National Institute of Standards and Technology, 1992.

[10] G. Hellwig. *Partial Differential Equations*. Blaisdell, New York, New York, 1964.

[11] M. Abramowitz and I. A. Stegun, editors. *Handbook of Mathematical Functions with Formulas, Graphs and Mathematical Tables*. National Bureau of Standards, Washington D.C., 1964.

[12] C. W. Gear. The simultaneous solution of differential-algebraic equations. *IEEE Trans. Circuit Theory*, 18:89–95, 1971.

[13] David Kahaner, Cleve Moler, and Stephen Nash. *Numerical Methods and Software*. Prentice Hall, Englewood Cliffs, New Jersey, 1989.

[14] Glenn P. Forney. Computing radiative heat transfer occurring in a zone fire model. Internal Report 4709, National Institute of Standards and Technology, 1991.

Nomenclature

c	specific heat wall segment material
K	thermal conductivity of wall segment material
$m_U(m_L)$	mass of upper (lower) layer
P	room pressure
q''	net heat flux
t	time
T_{amb}	ambient temperature
t_{final}	final simulation time
$u(x,t)$	temperature in a wall segment
x	position in wall segment
x_p	penetration depth
y	layer interface height
α	thermal diffusivity, $\alpha = \frac{K}{\rho c}$
Δt	time stepsize
Δx_i	breakpoint spacing
ρ	density of wall segment material

A Modeling Heat Conduction Using the Method of Lines

The standard MOL approach for solving the heat equation is to discretize the spatial variable by either replacing the spatial derivatives with finite difference approximations, or by expanding the unknown function as a linear combination of spatial basis functions with time dependent coefficients and deriving the ODE's *via* collocation. CONRAD1 uses the second approach and CONRAD2, the first. The MOL generally produces a stiff system of ODE's. Although this method was proposed many years before, it was not until the advent of stiff ODE solvers in the 1970's (see Gear [12]) that implementation of this method was practical.

For each wall segment there is an initial-boundary value problem which is coupled with the gas ODE's. These equations are

$$\frac{\partial u(x,t)}{\partial t} = \alpha \frac{\partial^2 u(x,t)}{\partial x^2}\ , \quad 0 < x < W, t > 0 \tag{10}$$

$$u(x,0) = T_{\text{amb}}\ , \quad 0 < x < W \tag{11}$$

$$-K\frac{\partial u}{\partial x}(0,t) = q''_{\text{convec}}(0,t) + q''_{\text{rad}}(0,t) \tag{12}$$

$$-K\frac{\partial u}{\partial x}(W,t) = q''_{\text{convec}}(W,t) + q''_{\text{rad}}(W,t)\ , \tag{13}$$

where $u(x,t)$ denotes the temperature at a distance x into the wall segment at time t and T_{amb} denotes the ambient temperature. The terms q''_{convec} and q''_{rad} denote the convective and radiative flux into the interior and exterior surfaces of the wall segments. Finally, $\alpha = \frac{K}{\rho c}$, where K, c, and ρ, denote the thermal conductivity, the specific heat, and the density of the segment material. The four gas ODE's are coupled to the above initial-boundary value problem by the dependencies of q''_{convec} and q''_{rad} on the gas layer temperatures T_L and T_U which can be determined from the gas solution variables. In addition, the energy transfer rates $\dot{q}_L$ and $\dot{q}_U$ to the lower and upper gas layers contain terms to account for the transfer of energy from the gas layers to the surfaces of the wall seqments *via* convection and radiation.

A.1 The Method of Lines Using the Piecewise Cubic Hermite Collocation Approach, CONRAD1

It is well-known in approximation theory that a function possessing four continuous derivatives on a closed, finite interval can be approximated to fourth order accuracy using piecewise cubic Hermite interpolation. This method of interpolation matches the function and its first derivative at a set of breakpoints. Between the breakpoints,

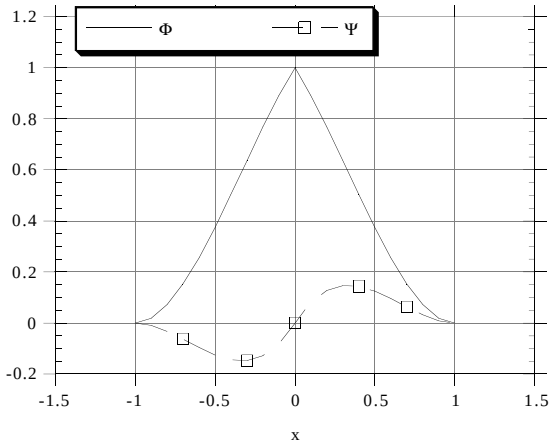

Figure 3: Plot of Cubic Hermite Basis Functions

the function is approximated by a cubic polynomial. The resulting approximation has a continuous first derivative (see [13]). Let ϕ_i and ψ_i denote the standard basis functions for piecewise cubic Hermite interpolation with breakpoints $x_1 < \ldots < x_{n_x}$. These basis functions have the defining properties

$$\begin{aligned} \psi_i'(x_j) &= \phi_i(x_j) = \delta_{ij} \\ \psi_i(x_j) &= \phi_i'(x_j) = 0 \end{aligned}$$

where δ_{ij} is the kroneker delta function with value zero unless $i = j$ in which case the value is one.

For the case where $x_1 = -1$, $x_2 = 0$, and $x_3 = 1$, the basis functions ϕ_2 and ψ_2 are plotted in Figure 3 and are given by

$$\begin{aligned} \phi_2(x) &= (|x| - 1)^2(2|x| + 1) \\ \psi_2(x) &= x(|x| - 1)^2 \end{aligned}$$

The MOL equations for CONRAD1 are derived by assuming that the wall segment temperature profiles have the form

$$u(x,t) = \sum_{i=1}^{n_x} [a_i(t)\phi_i(x) + b_i(t)\psi_i(x)] \; . \tag{14}$$

Equation (14) is then substituted into equation (10) to obtain

$$\sum_{i}^{n_x} \left(a_i'(t)\phi_i(x) + b_i'(t)\psi_i(x)\right) = \alpha \sum_{i}^{n_x} \left(a_i(t)\phi_i''(x) + b_i(t)\psi_i''(x)\right) \ . \tag{15}$$

Next, $2n_x - 2$ ODE's involving the $2n_x$ unknown coefficients, $a_i(t)$, $b_i(t)$, $i = 1, \ldots, n_x$, are derived by requiring that equation (15) be satisfied at the following two Gaussian points

$$\begin{aligned} p_{2j-1} &= x_j + \frac{3-\sqrt{3}}{6}(x_{j+1} - x_j), \\ p_{2j} &= x_{j+1} - \frac{3-\sqrt{3}}{6}(x_{j+1} - x_j) \end{aligned}$$

in each subinterval $j = 1, \cdots, n_x - 1$. The boundary conditions (12) and (13) provide two additional algebraic equations given by

$$\begin{aligned} -K[a_1(t)\phi_1'(0) + b_1(t)\psi_1'(0)] &= q''_{\text{convec}}(0,t) + q''_{\text{rad}}(0,t), \\ -K[a_{n_x}(t)\phi_{n_x}'(W) + b_{n_x}(t)\psi_{n_x}'(W)] &= q''_{\text{convec}}(W,t) + q''_{\text{rad}}(W,t). \end{aligned}$$

These discretizations lead to a system of $2n_x - 2$ ODE's and two algebraic equations of the form

$$A\frac{dy}{dt} = \alpha B y + F,$$

where A and B are $2n_x \times 2n_x$ matrices and y and F are $2n_x$ vectors. Analytic differentiation of the boundary conditions with respect to time, which would lead to a system of $2n_x$ ODE's, is not practical because the radiation flux terms in the boundary conditions are implicitly defined, nonlinear function of the gas variables, P, y, m_U, and m_L, and the wall segment surface temperatures. As a result the boundary conditions must be treated as algebraic equations. For $n_x = 4$ and $q'' = q''_{\text{convec}} + q''_{\text{rad}}$,

the vectors y and F have the form

$$y = \begin{pmatrix} a_1 \\ b_1 \\ a_2 \\ b_2 \\ a_3 \\ b_3 \\ a_4 \\ b_4 \end{pmatrix}, \quad F = \begin{pmatrix} \frac{q''(0,t)}{\rho c} \\ 0 \\ 0 \\ 0 \\ 0 \\ 0 \\ 0 \\ \frac{q''(W,t)}{\rho c} \end{pmatrix}$$

and the matrices A and B have the form

$$A = \begin{pmatrix} 0 & 0 & 0 & 0 & 0 & 0 & 0 & 0 \\ \phi_1(p_1) & \psi_1(p_1) & \phi_2(p_1) & \psi_2(p_1) & 0 & 0 & 0 & 0 \\ \phi_1(p_2) & \psi_1(p_2) & \phi_2(p_2) & \psi_2(p_2) & 0 & 0 & 0 & 0 \\ 0 & 0 & \phi_2(p_3) & \psi_2(p_3) & \phi_3(p_3) & \psi_3(p_3) & 0 & 0 \\ 0 & 0 & \phi_2(p_4) & \psi_2(p_4) & \phi_3(p_4) & \psi_3(p_4) & 0 & 0 \\ 0 & 0 & 0 & 0 & \phi_3(p_5) & \psi_3(p_5) & \phi_4(p_5) & \psi_4(p_5) \\ 0 & 0 & 0 & 0 & \phi_3(p_6) & \psi_3(p_6) & \phi_4(p_6) & \psi_4(p_6) \\ 0 & 0 & 0 & 0 & 0 & 0 & 0 & 0 \end{pmatrix} \tag{16}$$

and

$$B = \begin{pmatrix} 0 & 1 & 0 & 0 & 0 & 0 & 0 & 0 \\ \phi_1''(p_1) & \psi_1''(p_1) & \phi_2''(p_1) & \psi_2''(p_1) & 0 & 0 & 0 & 0 \\ \phi_1''(p_2) & \psi_1''(p_2) & \phi_2''(p_2) & \psi_2''(p_2) & 0 & 0 & 0 & 0 \\ 0 & 0 & \phi_2''(p_3) & \psi_2''(p_3) & \phi_3''(p_3) & \psi_3''(p_3) & 0 & 0 \\ 0 & 0 & \phi_2''(p_4) & \psi_2''(p_4) & \phi_3''(p_4) & \psi_3''(p_4) & 0 & 0 \\ 0 & 0 & 0 & 0 & \phi_3''(p_5) & \psi_3''(p_5) & \phi_4''(p_5) & \psi_4''(p_5) \\ 0 & 0 & 0 & 0 & \phi_3''(p_6) & \psi_3''(p_6) & \phi_4''(p_6) & \psi_4''(p_6) \\ 0 & 0 & 0 & 0 & 0 & 0 & 0 & 1 \end{pmatrix}. \quad (17)$$

The DAE solver DASSL by Petzold [7, 8] was chosen for use in CONRAD1 and CONRAD2. It is the most widely used production code for DAE's at this time. The following brief description of DASSL is taken from [7]. DASSL is a code for solving systems of DAE's of the form

$$F(t, y, y') = 0 \quad (18)$$
$$y(t_0) = y_0 \quad (19)$$
$$y'(t_0) = y_0', \quad (20)$$

where F, y, and y' are N-dimensional vectors. The basic idea for solving DAE systems using numerical ODE methods is to replace the derivative in (18) by a difference approximation, and then to solve the resulting system for the solution at the current time t_{n+1} using Newton's method. For example, replacing the derivative in (18) by the first order backward difference, we obtain the implicit Euler formula

$$F\left(t_{n+1}, y_{n+1}, \frac{y_{n+1} - y_n}{h_{n+1}}\right) = 0, \quad (21)$$

where $h_{n+1} = t_{n+1} - t_n$. This nonlinear system is then usually solved using some variant of Newton's method. The algorithms used in DASSL are an extension of this basic idea. Instead of always using the first order formula (21), DASSL approximates the derivative using the kth order backward differentiation formula, where k ranges from one to five. At every step it chooses the order k and the stepsize h_{n+1}, based on the behavior of the solution. DASSL can solve index zero and one systems. The

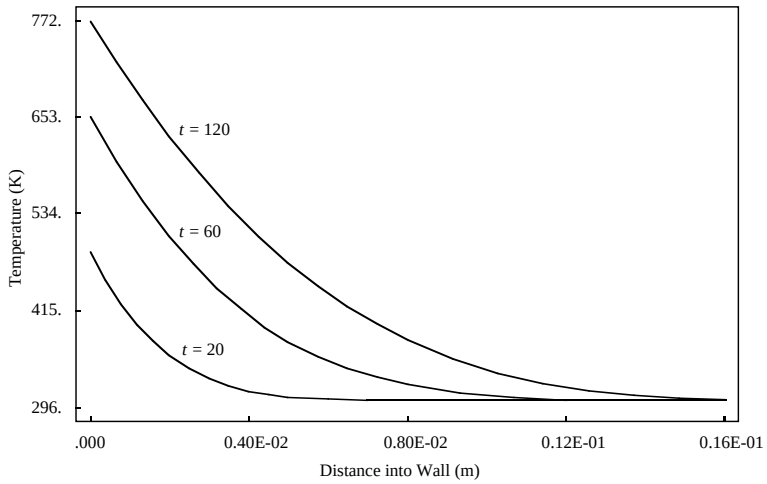

Figure 4: Ceiling Temperature Profiles at 20, 60 and 120 Seconds

index of the DAE system (18) is the minimum number of times that all or part of this system must be differentiated with respect to t in order to determine y' as a continuous function of y and t.

A.2 Graded Spatial Meshes

The MOL chooses the time discretization to maintain accuracy and stability, but the user must choose the spatial discretization. During the first seconds of a fire simulation, wall segment temperature profiles typically have steep gradients near the interior wall segment surfaces. Consequently, uniform meshes are not efficient. For both CONRAD1 and CONRAD2, graded meshes were developed with the grading dependent on the final simulation time t_{final}. These graded mesh were optimized for the case when the fire energy release rate takes a step jump at $t = 0$ and then is constant thereafter. In this case, the steepest temperature gradients occur near the interior surfaces of the wall segments. As the simulation evolves, these temperature profiles tend to flatten out. Figure 4 shows the ceiling temperature profiles at various times during a one room simulation. The room is 3 m long, 2 m wide, 3 m high and contains a 1 Mw fire on the floor. It has a single 1 m^2 vent to the outside. All conduction nodes are made from gypsum. The four-wall radiation model documented in [14] was used to model radiation heat transfer. The simulation runs for 2 minutes.

The general qualitative features of the profiles in Figure 4 are exhibited by the semi-infinite ($0 < x < \infty$) rod solution to the heat equation

$$u(x,t) = T_{\text{amb}} + (u_1 - T_{\text{amb}})\text{erfc}\left(\frac{x}{2\sqrt{\alpha t}}\right) , \tag{22}$$

where $u(0,t) = u_1$, a constant, the initial temperature is T_{amb}, $\alpha = \frac{K}{\rho c}$, and $\text{erfc}(x) = \frac{2}{\sqrt{\pi}} \int_x^\infty e^{-t^2} dt$ denotes the complementary error function. Using this solution as a guide, a graded mesh was developed to accommodate both short times and times near t_{final} using $n_x \geq 3$ breakpoints for CONRAD1 and $n_x \geq 10$ breakpoints for CONRAD2. In both cases $x_1 = 0$ and $x_{n_x} = W$. It is impossible for a fixed mesh to be optimum for all times $0 < t < t_{\text{final}}$. The meshes used in CONRAD1 and CONRAD2 were designed to concentrate most of the breakpoints between 0 and a breakpoint

$$x_b = \min(x_p, \frac{W}{2}) .$$

The point x_b was chosen to be the smaller of the midpoint of the wall segment, $W/2$, and the penetration depth, x_p, defined by

$$x_p := 2\sqrt{\alpha t_{\text{final}}}\,\text{erfc}^{-1}(.05) .$$

Table 2 gives penetration depths for several wall materials with $t_{\text{final}} = 600s$. To obtain penetration depths for a different t_{final}, multiply the values in column five of Table 2 by $\sqrt{t_{\text{final}}}$.

In CONRAD2, 80 percent of the breakpoints are to the left of x_b. The breakpoints on either side of x_b are quadratically graded so that they cluster near $x = 0$ and $x = W$.

The breakpoint design for CONRAD2 is somewhat different. For a fixed time $t > 0$, the heat equation solution in (22) is flattened out for $x > X(t) = 2\sqrt{\alpha t}\,\text{erfc}^{-1}(.05)$. To resolve the temperature profile at this time, a breakpoint should be placed near $X(t)$. Two of the breakpoints are generated this way. The breakpoint x_2 is the minimum of $X(t_{\text{print}})$ and $\frac{x_b}{4}$ with the $\frac{x_b}{4}$ term required to provide short time accuracy when t_{print} is not sufficiently small. CONRAD1 and CONRAD2 print out data every t_{print} seconds. The breakpoint x_{n_x-1} is set to x_b. By the time $X(t)$ has reached the ceiling midpoint, $\frac{W}{2}$, the temperature profile for $x > \frac{W}{2}$ is linear enough so that breakpoints at $\frac{W}{2}$ and W suffice.

Table 2: Penetration Depths, $t_{\text{final}} = 600s$

Material	K $(W/(mK))$	ρ (kg/m^3)	c $(Ws/(kgK))$	$2\sqrt{\alpha}\,\text{erfc}^{-1}(.05)$ (m^2/s)	x_p
Copper	387	380	8940	2.96×10^{-2}	0.72
Oak	.17	2380	800	8.28×10^{-4}	2.03×10^{-2}
PMMA	.19	1420	1190	9.29×10^{-4}	2.28×10^{-2}
Brick	.69	840	1600	1.99×10^{-3}	4.86×10^{-2}
Kaowool	.22	128	1047	3.55×10^{-3}	8.70×10^{-2}
Gypsum	.16	800	900	1.31×10^{-3}	3.20×10^{-2}
Concrete	1.75	2200	1000	2.47×10^{-3}	6.06×10^{-2}

B Heat Conduction in Multiple Slab Wall Segments

In this section methods are presented for handling the case of a wall segment composed of slabs of different materials. For simplicity, a two slab wall segment is examined.

B.1 The Heat Equation

For a two slab wall segment, the initial-boundary value problem defined in equations (3)–(6) must be replaced by the following interface problem. Find $u(x,t)$ so that

$$\frac{\partial u(x,t)}{\partial t} = \alpha^{(1)} \frac{\partial^2 u(x,t)}{\partial x^2},\ 0 < x < L < W,\ t > 0 \tag{23}$$

$$\frac{\partial u(x,t)}{\partial t} = \alpha^{(2)} \frac{\partial^2 u(x,t)}{\partial x^2},\ L < x < W,\ t > 0 \tag{24}$$

$$u(x,0) = T_{\text{amb}},\ 0 \le x \le W \tag{25}$$

$$u(0,t) = f_0(t),\ t \ge 0 \tag{26}$$

$$u(W,t) = f_1(t),\ t \ge 0 \tag{27}$$

$$u(L-,t) = u(L+,t) \tag{28}$$

$$-K^{(1)} \frac{\partial u^-}{\partial x}(L,t) = -K^{(2)} \frac{\partial u^+}{\partial x}(L,t)\ . \tag{29}$$

Here, $u(L-,t)$ and $u(L+,t)$ denote left and right hand limits, while $\frac{\partial u^-}{\partial x}$ and $\frac{\partial u^+}{\partial x}$ denote left and right hand derivatives. Material 1 occupies the interval $[0, L]$, while material 2 occupies the interval $[L, W]$. The interface conditions (28) and (29) required continuity of temperature and heat flux across the interface at $x = L$. Equation (29) assumes that there is no heat source embedded in the interface; this equation is derived from conservation of energy.

B.2 Finite Difference Equations

Introduce breakpoints $0 = x_1 < \ldots < x_n = W$, with $x_m = L$ for some m, $1 < m < n$, and let $\Delta x_j = x_{j+1} - x_j$. Let the temperature at breakpoint x_j at time t be denoted by $u_j(t)$. Replacing the second spatial derivative in the heat equations (23) and (24) by a second divided difference approximation and the first spatial derivative in equation (29) by a first divided difference approximation, yields the following DAE system:

$$u_j' = \alpha^{(1)} \frac{\frac{u_{j+1}-u_j}{\Delta x_j} - \frac{u_j - u_{j-1}}{\Delta x_{j-1}}}{\frac{\Delta x_j + \Delta x_{j-1}}{2}}, \; j = 2, \ldots, m-1 \tag{30}$$

$$u_j' = \alpha^{(2)} \frac{\frac{u_{j+1}-u_j}{\Delta x_j} - \frac{u_j - u_{j-1}}{\Delta x_{j-1}}}{\frac{\Delta x_j + \Delta x_{j-1}}{2}}, \; j = m+1, \ldots, n-1 \tag{31}$$

$$u_j(0) = T_{\text{amb}}, \; j = 1, \ldots, n \tag{32}$$

$$u_0 = f_0 \tag{33}$$

$$u_n = f_1 \tag{34}$$

$$-K^{(1)} \frac{u_m - u_{m-1}}{\Delta x_{m-1}} = -K^{(2)} \frac{u_{m+1} - u_m}{\Delta x_m} \; . \tag{35}$$

If the backward Euler method (see equation (21)) is used to advance the solution from time t to time $t + \Delta t$, the following tridiagonal linear system arises:

$$b_j u_{j-1}(t + \Delta t) + a_j u_j(t + \Delta t) + c_j u_{j+1}(t + \Delta t) = d_j \; . \tag{36}$$

The coefficients are as follows. For $j = 2, \ldots, m-1$,

$$\begin{aligned} b_j &= \frac{-2\alpha^{(1)}}{\Delta x_{j-1}(\Delta x_j + \Delta x_{j-1})} \\ a_j &= 1 + \frac{\alpha^{(1)}}{\Delta x_j \Delta x_{j-1}} \\ c_j &= \frac{-2\alpha^{(1)}}{\Delta x_j(\Delta x_j + \Delta x_{j-1})} \\ d_j &= u_j(t) \; . \end{aligned}$$

For $j = m+1, \ldots, n-1$,

$$\begin{aligned} b_j &= \frac{-2\alpha^{(2)}}{\Delta x_{j-1}(\Delta x_j + \Delta x_{j-1})} \\ a_j &= 1 + \frac{\alpha^{(2)}}{\Delta x_j \Delta x_{j-1}} \\ c_j &= \frac{-2\alpha^{(2)}}{\Delta x_j(\Delta x_j + \Delta x_{j-1})} \\ d_j &= u_j(t) \ . \end{aligned}$$

For $j = m$,

$$\begin{aligned} b_j &= -\frac{K^{(1)}}{\Delta x_{j-1}} \\ a_j &= -\frac{K^{(1)}}{\Delta x_{j-1}} + \frac{K^{(2)}}{\Delta x_j} \\ c_j &= \frac{K^{(2)}}{\Delta x_j} \\ d_j &= 0 \ . \end{aligned}$$

B.3 Cubic Hermite Expansion Equations

An expansion of the form (14) can be used for each slab. Introduce breakpoints $0 = x_1^{(1)}, \ldots, x_m^{(1)} = L$ and coefficients $a_j^{(1)}, b_j^{(1)}$ for the interval $[0, L]$, and introduce breakpoints $L = x_1^{(2)}, \ldots, x_{n-m+1}^{(2)} = W$ and coefficients $a_j^{(2)}, b_j^{(2)}$ for the interval $[L, W]$. Two DAE systems arise from applying the cubic Hermite collocation procedure of Section A.1 to equations (23), (25), and (26), and to equations (24), (25), and (27). These DAE systems are coupled by the interface conditions (28) and (29) which discretize as

$$\begin{aligned} a_m^{(1)}(t) &= a_1^{(2)}(t) \\ -K^{(1)} b_m^{(1)}(t) &= -K^{(2)} b_1^{(1)}(t) \ . \end{aligned}$$

NIST-114A
(REV. 3-90)

U.S. DEPARTMENT OF COMMERCE
NATIONAL INSTITUTE OF STANDARDS AND TECHNOLOGY

BIBLIOGRAPHIC DATA SHEET

1. PUBLICATION OR REPORT NUMBER
NISTIR 4886

2. PERFORMING ORGANIZATION REPORT NUMBER

3. PUBLICATION DATE
July 1992

4. TITLE AND SUBTITLE

Implicitly Coupling Heat Conduction into a Zone Fire Model

5. AUTHOR(S)

William F. Moss and Glenn P. Forney

6. PERFORMING ORGANIZATION (IF JOINT OR OTHER THAN NIST, SEE INSTRUCTIONS)

U.S. DEPARTMENT OF COMMERCE
NATIONAL INSTITUTE OF STANDARDS AND TECHNOLOGY
GAITHERSBURG, MD 20899

7. CONTRACT/GRANT NUMBER

8. TYPE OF REPORT AND PERIOD COVERED

9. SPONSORING ORGANIZATION NAME AND COMPLETE ADDRESS (STREET, CITY, STATE, ZIP)

10. SUPPLEMENTARY NOTES

11. ABSTRACT (A 200-WORD OR LESS FACTUAL SUMMARY OF MOST SIGNIFICANT INFORMATION. IF DOCUMENT INCLUDES A SIGNIFICANT BIBLIOGRAPHY OR LITERATURE SURVEY, MENTION IT HERE.)

This report examines several methods for coupling the partial differential equations that arise in conductive heat transfer with the ordinary differential equations that arise in zone fire modeling. Two existing algorithms (method of lines and time splitting) are discussed and a new strategy is proposed for performing this coupling. This strategy couples the wall surface temperature rather than the entire wall temperature profile with the other zone fire modeling solution variables by requiring that the wall surface temperature gradient and the incident heat flux (sum of convective and net radiative flux) satisfy Fourier's law, $q'' = -K\partial u/\partial x$.

Two prototype fire models were written to test the ideas discussed in this report. The first, CONRAD1, implements the method of lines strategy for solving heat conduction. The second, CONRAD2, implements the new strategy. Though inefficient, CONRAD1 uses well established numerical techniques and therefore serves as a benchmark to test the numerical ideas implemented in CONRAD2. Both programs use the stiff differential-algebraic equation solver DASSL. Supporting numerical results are presented.

12. KEY WORDS (6 TO 12 ENTRIES; ALPHABETICAL ORDER; CAPITALIZE ONLY PROPER NAMES; AND SEPARATE KEY WORDS BY SEMICOLONS)

conductive heat transfer; fire models; zone models; equations; computer models

13. AVAILABILITY

X	UNLIMITED
	FOR OFFICIAL DISTRIBUTION. DO NOT RELEASE TO NATIONAL TECHNICAL INFORMATION SERVICE (NTIS).
	ORDER FROM SUPERINTENDENT OF DOCUMENTS, U.S. GOVERNMENT PRINTING OFFICE, WASHINGTON, DC 20402.
X	ORDER FROM NATIONAL TECHNICAL INFORMATION SERVICE (NTIS), SPRINGFIELD, VA 22161.

14. NUMBER OF PRINTED PAGES
34

15. PRICE
A03

ELECTRONIC FORM